Hindawi
Shock and Vibration
Volume 2022, Article ID 1643050, 10 pages
https://doi.org/10.1155/2022/1643050

Research Article

Free Transverse Vibration of Circular Plate of Stepped Thickness with General Boundary Conditions by an Improved Fourier–Ritz Method

Qingjun Hao, Zhaobo Chen, and Wenjie Zhai

School of Mechatronics Engineering, Harbin Institute of Technology, Harbin 150001, China

Correspondence should be addressed to Zhaobo Chen; chenzb@hit.edu.cn

Received 14 March 2022; Accepted 31 May 2022; Published 23 June 2022

Academic Editor: Jean-Mathieu Mencik

In this investigation, free vibration of stepped circular Mindlin plate with arbitrary boundary conditions is presented by an improved Fourier–Ritz method. Based on the locations of the step variations, the stepped circular plate can be divided into different concentric annular and circular plates. The first-order shear deformation plate theory is employed to establish the theoretical model. Once all the displacements of a stepped circular plate are expanded by an improved Fourier series expansion, an exact solution can be obtained based on the Rayleigh–Ritz procedure by the energy function of the current model. The convergence and accuracy of the proposed method are proved by several numerical examples. The effects of classical boundary conditions and geometrical parameters on the frequency parameters of a stepped circular plate are also analyzed.

1. Introduction

The material of the potential savings is one of the most important design objectives in the fields of mechanical and aerospace engineering. Therefore, the stepped or variable plates are usually applied to reduce the plate weight and increase the stiffness of a structure. These structures with variable thickness endure dynamic loads induced by vibration and are thus difficult to analyze. Experimental research and numerical and analytical studies on isotropic and composite plates are available in the literature [1–3], whereas the studying works of literature on stepped plates, especially for stepped circular or annular plates, are limited. Thus, this paper aims to solve the free vibration behavior of stepped circular plates with general boundary conditions by a semianalytical numerical method called the improved Fourier–Ritz approach.

The stepped thickness plates can be divided into rectangular and circular/annular plates with stepped thickness variations. There is a great range of works of literature that have been studied on free vibration of different kinds of plates with variable thickness, where the semianalytical or numerical solution procedure and classical plate theory (CPT) are mostly used. By dividing the steeped beams and rectangular plates into elemental substructures and using dynamic Green's function to express the displacements, Lee and Bergman [4] obtained the forced vibration of the system. Juarez [5] analyzed the axisymmetric vibration of circular plates with only one step by the classical plate solution method. Based on the finite strip method (FSM), which was presented by Cheung [6], Guo et al. [7] developed this method with a dynamic function instead of the static shape function in FSM and, thus, obtained efficient methods for the vibration analysis of stepped thickness rectangular plates to guarantee higher-order modes accurate enough. Chopra [8] obtained an exact method to research the vibration characteristics of a simply supported rectangular plate with stepped thickness. Xiang and Wang [9] proposed an analysis method based on the state-space technique and the Levy method to acquire exact buckling and vibration solutions of rectangular plates with one or two stepped thickness. Subsequently, Xiang and Zhang [10] developed an analytic technique involving the domain decomposition method to solve the vibration problem of an annual and circular plate with stepped thickness variation. Duan et al. [11] researched the free transverse vibration of a circular plate with uniform

and stepped thickness with a method of discrete singular convolution, which avoids singularity at the circular plate center point without regularity conditions needed. Ghannadiasl and Mofid [12] introduced the green function method to analyze the free vibration of stepped circular plates with arbitrary elastic foundations and the internal elastic support ring. Avalos et al. [13] investigated the free vibration of annular plates of stepped thickness with the inner edge free and the outer boundary elastically constrained by the optimized Rayleigh–Ritz method. By the Ritz method, Bhardwaj et al. [14] surveyed the problem of the vibration analysis of a circular plate with two-dimensional thickness variations, yet the boundary conditions for the plate model are confined to clamped and simply supported ones. Gupta and Bhardwaj [15] studied free transverse vibration of thin circular plates with a quadratically variable thickness on Winkler elastic foundation by classical plate theory and the Rayleigh–Ritz method. By the modified couple stress theory and Hamilton's principle, Eshraghi et al. [16] investigated static bending and free vibration problems involving thermally loaded functionally graded annular and circular microplates. Then, Eshraghi and Dag [17] developed a new domain-boundary element formulation to investigate the axis-symmetric dynamic response of functionally graded circular and annular Mindlin plates with through-the-thickness variations of physical properties. Lam and Amrutharaj [18] employed a novel hybrid method to analyze the natural frequencies of a rectangular plate with stepped thickness variations and different edge boundary conditions, which had incorrect continuity conditions at stepped sections as was proposed by Dickinson [19]. Rajasekaran and Wilson [20] applied the well-known finite difference method to analyze the vibration frequencies and exact buckling loads for isotropic plates with variable thicknesses. Recently, Cho et al. [21] applied the assumed mode method to simplify the dynamic analysis of stiffened panels and stepped-thickness rectangular Mindlin plates with general boundary conditions. Derakhshani et al. [22] presented an exact solution to analyze the free vibration of stepped circular/annular functionally graded plates via the Mindlin plate theory.

A review of the above papers reveals that most of the previous researches on free vibrations of stepped rectangular and circular plates are confined to the classical boundary conditions and their combinations. Many of the existing solution methods are defined to solve a specific set of different boundary conditions, and thus, the solution procedures are calculated by modifying the trial functions to adapt to different boundary conditions. In this paper, an improved Fourier–Ritz method, which is proposed by Li et al. to solve vibrations of a single beam [23, 24] or plate [25–29], is used to solve the transverse vibration of a stepped circular plate with general boundary conditions. The transverse vibration of a stepped circular plate can also be expressed as combinations of Fourier cosine series and sine series functions. Compared to the existing solution methods, the transverse vibration of a stepped circular plate under different boundary conditions can be easily obtained just by changing the stiffness of the three sets of springs at the outer edge without altering the solution procedures. In order to illustrate the convergence and accuracy of this method, the current results are compared with those results of other published papers. The effects of geometric parameters of the research model on frequency parameters are discussed. Some new results for the transverse vibration of a stepped circular plate with classical conditions are presented.

2. Theoretical Formulations

2.1. Description of the Model. The stepped circular Mindlin plate with m steps Radii $R_1, R_2, \ldots, R_m(=b)$ and stepped thicknesses $h_1, h_2, \ldots, h_m$ considered in this paper, along with the specified coordinate system (r, θ, z), is shown in Figure 1, where the plate dimensions and geometry are defined for the extraction of mathematical formulas. At the outer edge of the considered stepped circular Mindlin plate, the boundary conditions can be expressed as the combinations of various linear and torsional springs. Based on the first-order shear deformation, all kinds of boundary conditions can be expressed by defining the stiffness of one linear spring (k_b^w) as well as the two torsional springs (K_b^r, K_b^θ). For example, the stepped circular Mindlin plate model with simply supported boundary conditions can be obtained by setting the linear spring to infinite values (usually represented by very high values 10^{13} or higher in actual calculations) and the two torsional springs to 0 (under the free boundary conditions, usually represented by relatively very small values 10 to avoid singular matrix problems in actual calculations). In this way, all different boundary conditions, including the classical and elastic boundaries as well as their combinations, can be expressed by setting the values of linear and torsional spring stiffness.

2.2. Kinematic Relationship and Stress-Strain Relations. Based on the first-order shear deformation plate theory, the assumed displacement for the ith segment of the stepped circular Mindlin plate, as shown in Figure 1, can be defined as

$$u_{ir}(r, \theta, z, t) = -z\phi_{ir}(r, \theta, t), \tag{1}$$

$$u_{i\theta}(r, \theta, z, t) = -z\phi_{i\theta}(r, \theta, t), \tag{2}$$

$$u_{iz}(r, \theta, z, t) = w_{ir}(r, \theta, t), \tag{3}$$

where u_{ir}, $u_{i\theta}$, and u_{iz} indicate the displacement for the ith segment of the stepped circular Mindlin plate in r, θ, and z directions. ϕ_{ir} and $\phi_{i\theta}$ are the rotations of the normal to the neutral surface on the r and θ direction, respectively.

Considering the relationship between small deformation and linear strain displacement, the curvature changes components, denoted by ε_{ir}, $\varepsilon_{i\theta}$, ε_{iz}, γ_{irz}, $\gamma_{ir\theta}$, and $\gamma_{i\theta z}$, for the ith segment of the model on the middle surface can be obtained as

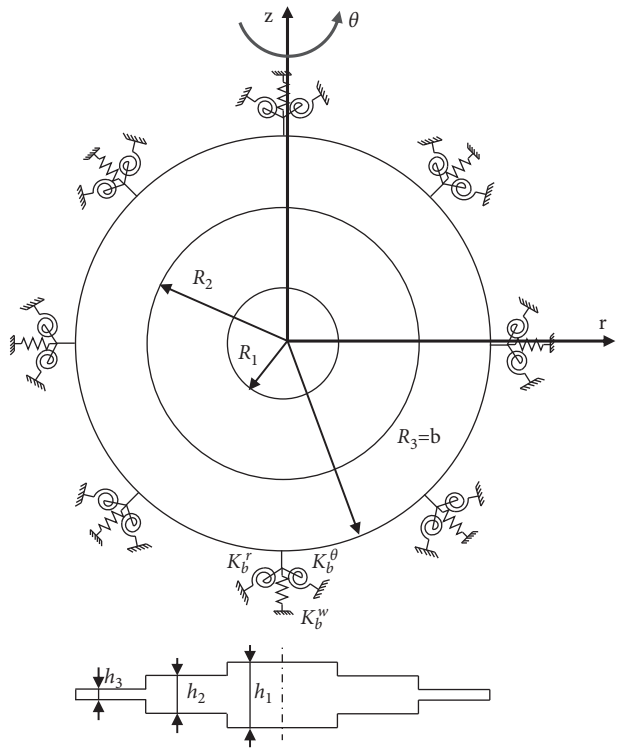

Figure 1: Geometry model and coordinate system for stepped circular Mindlin plate.

$$\varepsilon_{\mathrm{ir}} = \frac{\partial u_{ir}}{\partial r} \qquad \varepsilon_{i\theta} = \frac{\partial u_{i\theta}}{r\,\partial\theta} + \frac{u_{ir}}{r}$$

$$\varepsilon_{\mathrm{iz}} = \frac{\partial w_{ir}}{\partial z} \qquad \gamma_{irz} = \frac{\partial w_{ir}}{\partial r} + \frac{\partial u_{ir}}{\partial z}. \tag{4}$$

$$\gamma_{ir\theta} = \frac{\partial u_{ir}}{r\,\partial\theta} + \frac{\partial u_{i\theta}}{\partial r} - \frac{u_{i\theta}}{r} \qquad \gamma_{i\theta z} = \frac{\partial w_{ir}}{r\,\partial\theta} + \frac{\partial u_{i\theta}}{\partial z}$$

According to Hook's law and considering the Mindlin plate theory, the stress-strain relationship for the ith segment of the considered model by elastic theory, as shown in Figure 1, can be expressed as

$$\begin{bmatrix} \frac{E}{1-v^2} & \frac{vE}{1-v^2} & 0 & 0 & 0 \\ \frac{vE}{1-v^2} & \frac{E}{1-v^2} & 0 & 0 & 0 \\ 0 & 0 & G & 0 & 0 \\ 0 & 0 & 0 & \kappa G & 0 \\ 0 & 0 & 0 & 0 & \kappa G \end{bmatrix} \begin{bmatrix} \varepsilon_{ir} \\ \varepsilon_{i\theta} \\ \gamma_{ir\theta} \\ \gamma_{irz} \\ \gamma_{i\theta z} \end{bmatrix} = \begin{bmatrix} \sigma_{ir} \\ \sigma_{i\theta} \\ \tau_{ir\theta} \\ \tau_{irz} \\ \tau_{i\theta z} \end{bmatrix}, \tag{5}$$

where σ_{ir} and $\sigma_{i\theta}$ are the normal stresses, $\tau_{ir\theta}$, τ_{irz}, and $\tau_{i\theta z}$ are the shear stresses for the ith segment of a stepped circular plate, E, G, κ, and v are the young's modulus, shear modulus, shear correction factor, and Poisson's ratio of the considered model, respectively.

Based on equations (1)–(5), the normal and shear strains for the ith segment of the considered stepped circular Mindlin plate can be written as follows:

$$\begin{bmatrix} \varepsilon_{\mathrm{ir}} \\ \varepsilon_{i\theta} \\ \gamma_{\mathrm{ir}\theta} \\ \gamma_{\mathrm{irz}} \\ \gamma_{i\theta z} \end{bmatrix} = \begin{bmatrix} -z\frac{\partial \phi_{ir}}{\partial r} \\ -z\left(\frac{\partial \phi_{i\theta}}{r\,\partial\theta} + \frac{\phi_{ir}}{r}\right) \\ -z\left(\frac{\partial \phi_{ir}}{r\,\partial\theta} + \frac{\partial \phi_{i\theta}}{\partial r} - \frac{\phi_{i\theta}}{r}\right) \\ \frac{\partial w_{ir}}{\partial r} - \phi_r \\ \frac{\partial w_{ir}}{r\,\partial\theta} - \phi_\theta \end{bmatrix}. \tag{6}$$

2.3. Energy Expressions. According to Mindlin's theory of moderate thick plate, the maximum strain energy for the ith segment of the stepped circular plate in Figure 1 can be expressed as

$$U_i = \frac{1}{2}\iiint_{V_i} \left(\sigma_{ir}\varepsilon_{ir} + \sigma_{i\theta}\varepsilon_{i\theta} + \tau_{ir\theta}\gamma_{ir\theta} + \tau_{irz}\gamma_{irz} + \tau_{i\theta z}\gamma_{i\theta z}\right) r\,\mathrm{d}r\,\mathrm{d}\theta\,\mathrm{d}z. \tag{7}$$

Substituting equations (5) and (6) into (7), the strain energy of the considered model can be written in terms of displacement and rotations of the middle surface.

$$U_i = \frac{E}{2\left(1-v^2\right)} \times \frac{h_i^3}{12} \iint \left(\frac{\partial \phi_{ir}}{\partial r} + \frac{\partial \phi_{i\theta}}{r\,\partial \theta} + \frac{\phi_{ir}}{r} \right)^2 r\, dr\, d\theta + \frac{1}{2} \times \frac{h_i^3 G}{12} \iint \left(\frac{\partial \phi_{ir}}{r\,\partial \theta} + \frac{\partial \phi_{i\theta}}{\partial r} - \frac{\phi_{i\theta}}{r} \right)^2 r \mathrm{d}r\mathrm{d}\theta + \frac{1}{2} \kappa G h_i \iint \left[\left(\frac{\partial w_{ir}}{\partial r} - \phi_{ir} \right)^2 + \left(\frac{\partial w_{ir}}{r\,\partial \theta} - \phi_{i\theta} \right)^2 \right] r \mathrm{d}r\mathrm{d}\theta. \tag{8}$$

The kinetic energy for the ith segment of the considered stepped circular plate is given by

$$T_i = \frac{1}{2} \iiint_{V_i} \rho \left[\left(\frac{\partial u_{ir}}{\partial t} \right)^2 + \left(\frac{\partial u_{i\theta}}{\partial t} \right)^2 + \left(\frac{\partial u_{iz}}{\partial t} \right)^2 \right] r \mathrm{d}r\mathrm{d}\theta\mathrm{d}z. \tag{9}$$

The strain potential energy of boundary springs for stepped annular plate in Figure 1 can be defined as follows:

$$\mathrm{U}_{sp} = \frac{1}{2} \int_0^{2\pi} \left(k_b^w w_b^2 + \mathrm{r_b} \phi_{br}^2 + \mathrm{b}_\theta \phi_{b\theta}^2 \right) b \mathrm{d}\theta. \tag{10}$$

In order to ensure the displacement coordination of adjacent interfaces, a group of linear coupling springs and two groups of torsional coupling springs are introduced here. Therefore, interface potential energy between the ith and $(i+1)$th segments in Figure 1 can be defined as follows:

$$\prod_{i,i+1}^{\lambda} = \frac{1}{2} \int_0^{2\pi} \left(\widetilde{K}_i^r \vartheta_{iu}^2 + \widetilde{K}_i^\theta \vartheta_{iv}^2 + \widetilde{k}_i^w \vartheta_{iv}^2 \right) R_i \mathrm{d}\theta, \tag{11}$$

where

$$\begin{aligned} \vartheta_{iu} &= \phi_{ir} - \phi_{(i+1)r}, \\ \vartheta_{iv} &= \phi_{i\theta} - \phi_{(i+1)\theta}, \\ \vartheta_{iw} &= w_{ir} - w_{(i+1)r}. \end{aligned} \tag{12}$$

In this formulation, the kinematic and physical compatibility conditions between the two computational meridians of $\theta = 0$ and $\theta = 2\pi$ are required to guarantee the continuities of the displacement and their derivatives of the considered model. The modified potential energy is introduced to incorporate the continuity conditions, given as

$$\prod_{i}^{cp} = \frac{1}{2} \int_{R_i}^{R_{i+1}} \left[K_i^r \vartheta_{iu}'^2 + K_i^\theta \vartheta_{iv}'^2 + k_i^{w\prime}{}_{iw} \right] \mathrm{d}r, \tag{13}$$

where

$$\begin{aligned} {}^{iu}_{\vartheta} &= \phi_{ir} \mid_{\theta=0} - \phi_{ir} \mid_{\theta=2\pi}, \\ {}^{iv}_{\vartheta} &= \phi_{i\theta} \mid_{\theta=0} - \phi_{i\theta} \mid_{\theta=2\pi}, \\ {}^{iw}_{\vartheta} &= w_{ir} \mid_{\theta=0} - w_{ir} \mid_{\theta=2\pi}. \end{aligned} \tag{14}$$

ϑ_{iu}, ϑ_{iv}, and ϑ_{iw} are the essential continuity equations on the common boundary between adjacent segments (i) and $(i+1)$ in Figure 1, and ${}^{iu}_{\vartheta}$, ${}^{iv}_{\vartheta}$, and ${}^{iw}_{\vartheta}$ represent the essential continuity equations between the two computational meridians of $\theta = 0$ and $\theta = 2\pi$ corresponding to the i th segment.

2.4. Solution Procedures. As shown in Figure 1, a stepped circular Mindlin plate with n steps could be divided into n annular or circular Mindlin plates. An annular or circular plate of radius r_i and thickness h_i, which refers to the ith segment of the model as depicted in Figure 1, is considered here. It is well known that the accuracy and convergence solutions depend on the method of selecting suitable admissible functions in the Rayleigh–Ritz equation. There are two conditions that must be satisfied when choosing the permissible functions of equations. Firstly, the permissible functions must be integrable, differential, continuous, and linearly independent. Secondly, the permissible functions must satisfy the boundary conditions. Therefore, it is important to construct appropriate admissible displacement functions in the current research. In order to ensure the accuracy and accelerate the convergence of the constructed series expansion, a new form of trigonometric series expansions with four sine series is introduced here, and the detailed expression for the transverse displacement and rotation components can be obtained as follows [27, 29]:

$$\phi_{ir} = \sum_{m,n=-4}^{\infty} A_{mn}^i \phi_{im}(s) \phi_{in}(\theta), \tag{15}$$

$$\phi_{i\theta} = \sum_{m,n=-4}^{\infty} B_{mn}^i \phi_{im}(s) \phi_{in}(\theta), \tag{16}$$

$$w_{ir} = \sum_{m,n=-4}^{\infty} C_{mn}^i \phi_{im}(s) \phi_{in}(\theta), \tag{17}$$

where

$$\varphi_{im}(s) = \begin{cases} \cos\left(\dfrac{m\pi s}{R_i} \right) & m \geq 0, \\ \sin\left(\dfrac{m\pi s}{R_i} \right) & m < 0, \end{cases} \qquad \varphi_{in}(\theta) = \begin{cases} \cos\left(\dfrac{n\theta}{2} \right) & n \geq 0, \\ \sin\left(\left(\dfrac{n\theta}{2} \right) \right) & n < 0. \end{cases} \tag{18}$$

After expressing the potential energy and kinetic energy, all the assumed displacement functions are inserted into the potential and kinetic energy equations, which are then further minimized relative to the expansion coefficient in the

displacement field. Mathematically, the Lagrangian for the steeped circular Mindlin plate can generally be expressed as

$$L = \sum_{i}\left(T_i - U_i - \prod_{i}^{cp} - \prod_{i,i+1}^{\lambda}\right) - U_{sp}. \tag{19}$$

Substituting equations (15)–(17) into equations (8)–(11) and (13), and then minimizing Lagrangian equation (19) against all the unknown series expansion coefficients, specifically

$$\frac{\partial L}{\partial \vartheta} = 0, \quad \vartheta = A_{mn}^{i}, B_{mn}^{i}, C_{mn}^{i}, \tag{20}$$

where ϑ represents the unknown coefficients A_{mn}^{i}, B_{mn}^{i}, and C_{mn}^{i}. The acceptable precision is acquired by properly setting the truncated number $m = M$ and $n = N$, and the motion of the considered stepped circular Mindlin plate is obtained, which is given by the following matrix:

$$\left(K - \omega^2 M\right)G = 0, \tag{21}$$

where

$$G = \left\{G^1, G^2, \ldots G^i \ldots G^k, \right\}.$$

$$G^i = \begin{Bmatrix} A_{-4,-4}^{i}, A_{-4,-3}^{i}, \ldots, A_{-m,-4}^{i}, A_{-m,-3}^{i} \ldots, A_{mn}^{i}, \ldots A_{MN}^{i} \\ B_{-4,-4}^{i}, B_{-4,-3}^{i}, \ldots, B_{-m,-4}^{i}, B_{-m,-3}^{i}, \ldots, B_{mn}^{i}, \ldots B_{MN}^{i} \\ C_{-4,-4}^{i}, C_{-4,-3}^{i}, \ldots, C_{-m,-4}^{i}, C_{-m,-3}^{i}, \ldots, C_{mn}^{i}, \ldots C_{MN}^{i} \end{Bmatrix}. \tag{22}$$

For the analysis of the free transverse vibration characteristics of the stepped circular plate, the eigenvalues and eigenvectors can be easily obtained by solving the standard matrix of equation (21). The physical modal shape can be readily yielded by substituting the corresponding eigenvectors into equations (15)–(17) for the given natural frequency.

3. Numerical Examples and Discussions

In this section, the convergence and accuracy of the proposed method are proved by several numerical examples, and the results are compared with those published by other scholars using traditional methods. Then, the stepped circular Mindlin plates with various boundary restraints are studied. Lastly, the influence of geometric parameters on frequency parameters for the research model is reported.

3.1. The Convergence and Accuracy Analysis. A stepped circular Mindlin plate with simply supported boundary conditions is adopted here to illustrate the accuracy and convergence of the solving method as mentioned in the precious section.

It is easy to obtain the boundary conditions of the calculated model just by setting the stiffness of the one linear spring and two torsional springs to a value of 10 or smaller. The first five natural frequencies are calculated by equation (21) with different truncation numbers M and N of the improved Fourier methods and then compared with published literature [10, 13]. The basic material and geometric parameters used for calculation are given as follows:

$$\rho = \frac{7850kg}{m^3},$$

$$E = 2.1 \times 10^{11} Pa \mu = 0.3, \tag{23}$$

$$b = 1m, \frac{h_2}{b} = 0.005 \frac{h_1}{h_2} = 2.$$

Table 1: The first five natural frequencies $\Omega = \omega b^2 \sqrt{\rho h_2 / D_2}$ with M and N increasing.

M and N	Modal number				
	1	2	3	4	5
6	5.769	35.071	88.091	169.129	264.358
8	5.764	35.067	88.087	169.118	264.342
10	5.760	35.061	88.080	169.110	264.338
15	5.758	35.058	88.078	169.106	264.333
20	5.758	35.058	88.077	169.106	264.332
Xiang and Zhang [10]	5.75819	35.0577	88.07734	169.105	264.323
Avalos et al. [13]	5.82394	35.0578	89.6624	169.730	269.625

As a powerful method, Table 1 also indicates good accuracy and convergence rate. The frequency parameters decrease rapidly with the truncation number M and N increase. When the truncation configuration is 10, the worst case is 0.035% compared with the truncation configuration 15 and 20, which is acceptable. Thus, the calculation truncation number is set as 15 for the following number calculations.

The values in brackets (k, p) denote the number of nodal diameter k and the mode sequence p for a given k value [11].

Figure 2 shows the first four modal shapes of the stepped circular plate with simply supported boundary conditions. As shown in the literature [5], in order to show the influence of thickness variation on modal shape smoothness clearly, the curves in Figure 2 all vary along the radial coordinate. All four modal shapes are normalized by a multiplication factor $|1/w(\mathrm{r})_{\max}|$. It is easy to find out that the step variation in the considered plate almost has no effect on the modal shape smoothness of the stepped circular plate, and the transverse displacement has well smooth at the location of step variation.

3.2. Steeped Circular Mindlin Plates with Various Boundary Restraints. In this subsection, the free transverse vibration of stepped circular Mindlin plate with various classical boundary conditions is carried out to prove the universality of the presented method. Tables 2–4 show the nondimensional frequency parameters $\Omega = \omega b^2 \sqrt{\rho h_2 / D_2}$ of the current model with free, simply supported, and clamped boundary conditions. The geometric parameters of the considered model, including the location of the step variation, plate thickness ratio, and step thickness ratios, are given as $h_1/b = 0.1$, $r_1/b = 0.5$, $h_1/h_2 = 0.4, 0.8, 1.5$. In these

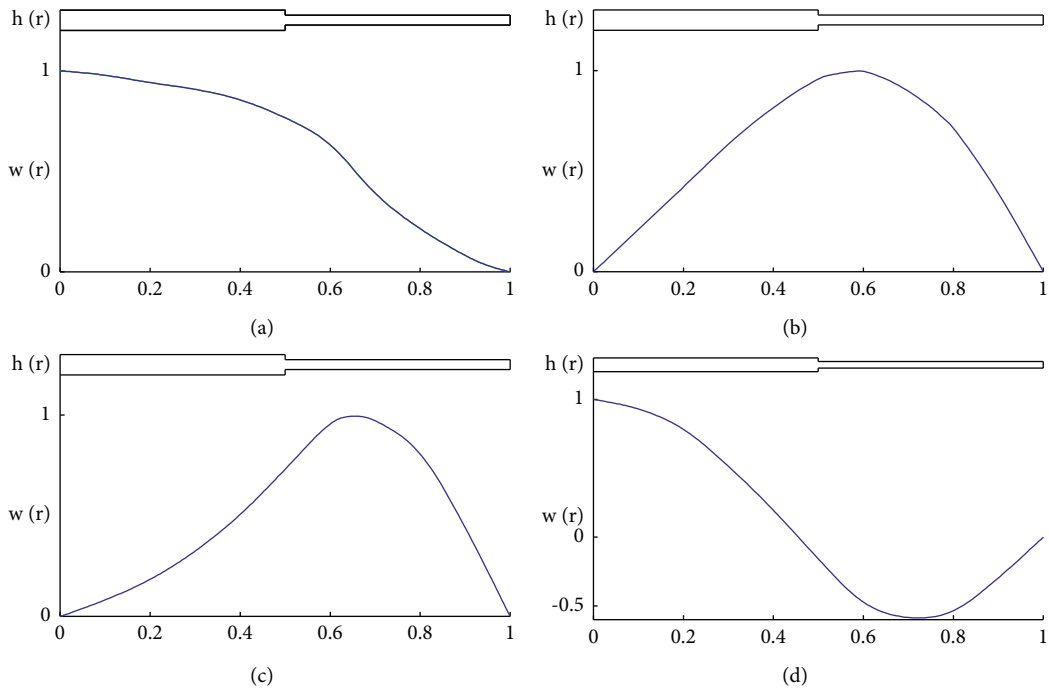

Figure 2: Modal shapes of transverse displacement for stepped circular Mindlin plate with simply supported boundary condition. (a) First mode$(k, p) = (0, 1)$, (b) second mode$(k, p) = (1, 1)$, (c) third mode$(k, p) = (2, 1)$, (d) fourth mode$(k, p) = (0, 2)$.

Table 2: Dimensionless frequency parameters $\Omega = \omega b^2\sqrt{\rho h_2/D_2}$ for stepped circular Mindlin plate with free boundary condition ($\upsilon = 0.3$).

h_1/h_2	Modal number	Present	FEM	Xiang and Zhang [10]
0.4	1	4.352	4.355	—
	2	6.528	6.532	—
	3	11.015	11.020	—
	4	14.602	14.606	—
	5	15.192	15.198	—
0.8	1	4.876	4.880	—
	2	8.623	8.627	—
	3	11.641	11.647	—
	4	18.371	18.378	—
	5	21.534	21.542	—
1.5	1	6.892	6.898	6.88138
	2	11.432	11.440	11.4342
	3	13.386	13.493	13.3881
	4	21.672	21.681	21.6542
	5	22.268	22.380	22.2602

Table 3: Dimensionless frequency parameters $\Omega = \omega b^2\sqrt{\rho h_2/D_2}$ for stepped circular Mindlin plate with simply supported boundary condition ($\upsilon = 0.3$).

h_1/h_2	Modal number	Present	FEM	Xiang and Zhang [10]
0.4	1	4.016	4.021	—
	2	9.875	9.881	—
	3	19.085	19.090	—
	4	20.012	20.021	—
	5	32.517	32.529	—
0.8	1	4.692	4.698	—
	2	12.276	12.282	—
	3	22.135	22.134	—
	4	27.256	27.265	—
	5	37.635	37.647	—
1.5	1	5.671	5.679	5.68854
	2	14.483	14.490	14.4923
	3	27.012	27.021	26.9433
	4	32.685	32.696	32.6687
	5	41.198	41.208	41.1944

numerical calculations, the current solutions are validated by published literature [10] and the FEM results. It is easily seen that as the plate thickness ratio increases, the nondimensional frequency parameters also increase due to the effect of rotary inertia and transverse shear deformation, which conforms to our common sense.

3.3. Parametric Study. In this subsection, the effects of geometrical parameters on the frequency parameters of the stepped circular Mindlin plate are analyzed by the numerical model established in the previous section. Figure 3–5 shows the relationship between the nondimensional frequency parameters $\Omega = \omega b^2\sqrt{\rho h_2/D_2}$ of the current model with classical boundary conditions and the variation of the step location r_1/b. The geometric parameters of the considered model, including plate thickness ratio and step thickness ratio, are given as $h_1/b = 0.006, 0.15$, $h_1/h_2 = 2$.

Figure 3shows that the first two-order frequency parameters of the free stepped circular plate increase first and then decrease within the considered range of the step location ratio. Nevertheless, the variation trend of the third and fourth frequency parameters tends to be increasing directly. Figures 4 and 5 show that all the considered

Table 4: Dimensionless frequency parameters with $\Omega = \omega b^2\sqrt{\rho h_2/D_2}$ for stepped circular Mindlin plate with clamped boundary condition ($\upsilon = 0.3$).

h_1/h_2	Modal number	Present	FEM	Xiang and Zhang [10]
0.4	1	10.125	10.129	—
	2	17.014	17.021	—
	3	23.562	23.570	—
	4	27.450	27.462	—
	5	39.128	39.140	—
0.8	1	10.067	10.073	—
	2	19.138	19.145	—
	3	30.019	30.025	—
	4	32.816	32.823	—
	5	46.235	46.242	—
1.5	1	10.652	10.658	10.6655
	2	21.713	21.719	21.7095
	3	35.486	35.495	35.0502
	4	41.583	41.591	41.5770
	5	50.386	50.397	50.3801

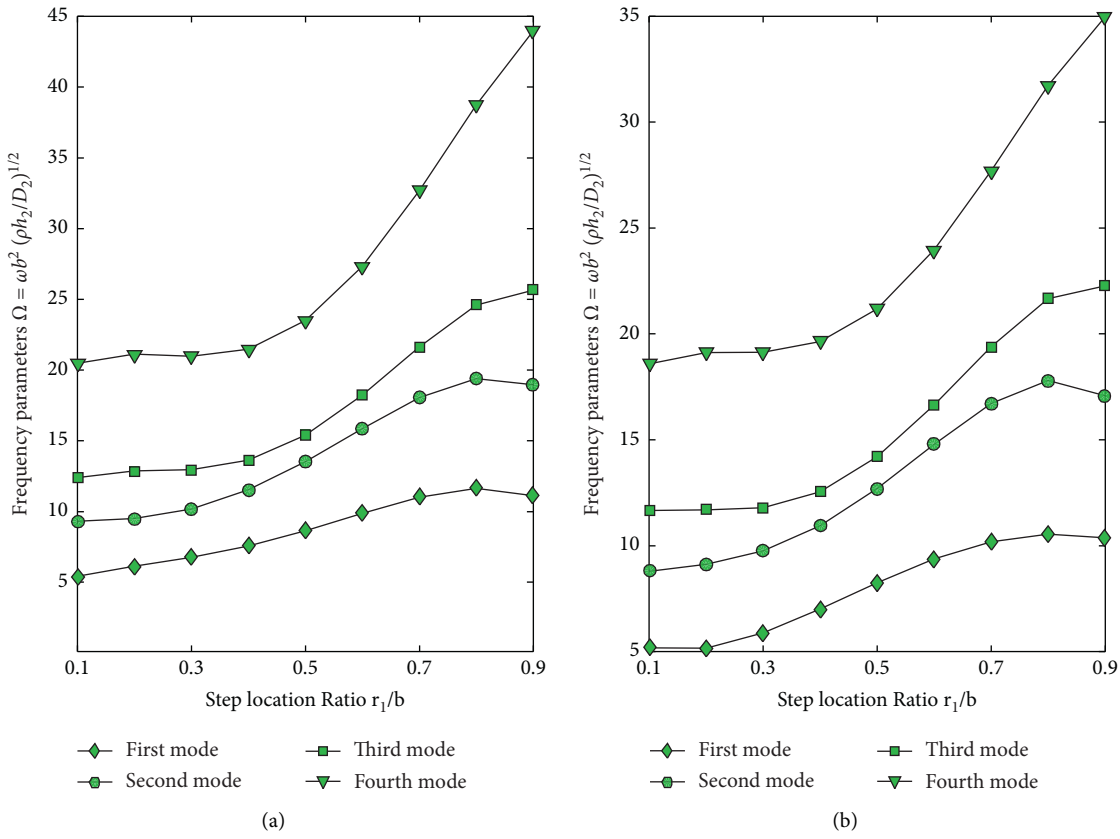

Figure 3: Frequency parameters $\Omega = \omega b^2\sqrt{\rho h_2/D_2}$ versus step location ratio r_1/b for free stepped circular Mindlin plates, step thickness ratio $h_1/h_2 = 2$, and plate thickness ratios h_1/b = (a) 0.006 and (b) 0.15.

frequency parameters for the current model present a monotonous increasing trend and the frequency parameter for the first mode manifests an insignificant growth trend as the step location ratio increases.

Figure 6 shows the relationship between the nondimensional frequency parameters $\Omega = \omega b^2\sqrt{\rho h_2/D_2}$ of the current model with three kinds of classical boundary conditions and the variation of the step thickness ratio h_1/h_2. The geometric parameters of the research model are given as $r_1/b = 0.4$, $h_1/b = 0.1$. Except for the first and second modes of the simply supported and clamped stepped circular plate, all the considered frequency parameters have an obvious increasing trend as the step thickness ratio increases. The considered frequency parameters for the second mode of

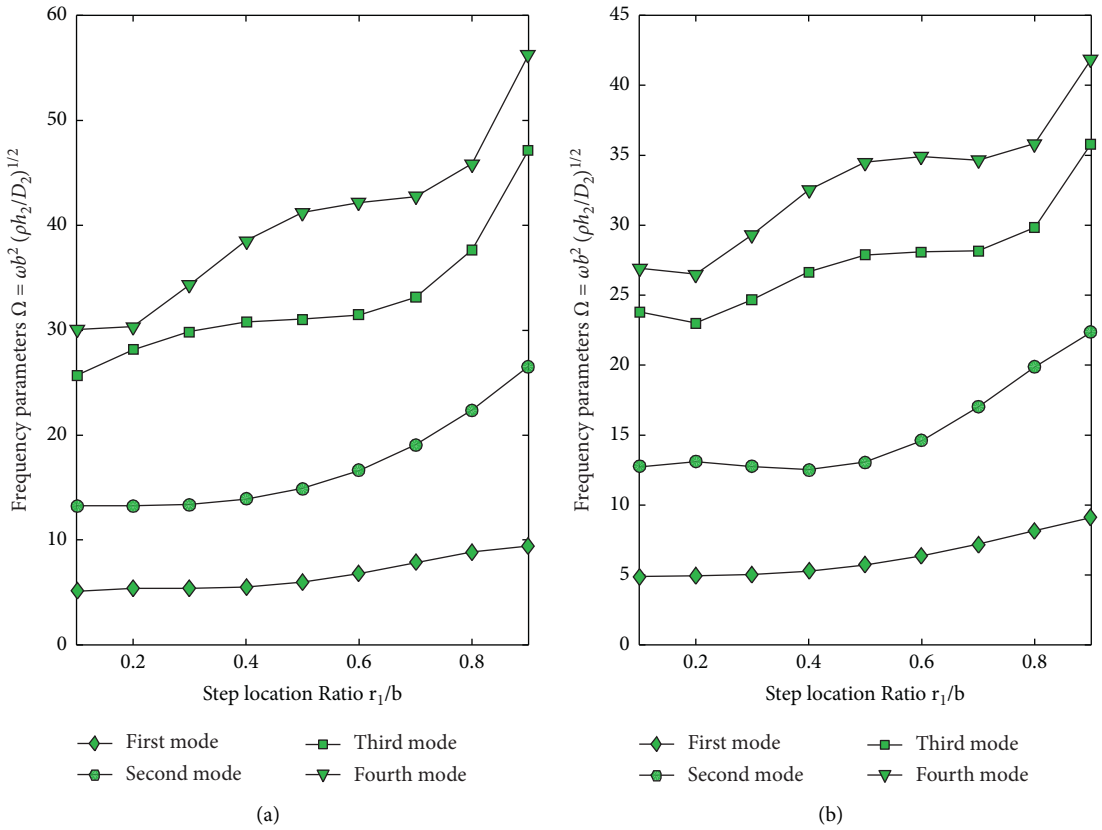

FIGURE 4: Frequency parameters $\Omega = \omega b^2 \sqrt{\rho h_2/D_2}$ versus step location ratio r_1/b for simply supported stepped circular Mindlin plates, step thickness ratio $h_1/h_2 = 2$, and plate thickness ratios h_1/b = (a) 0.006 and (b) 0.15.

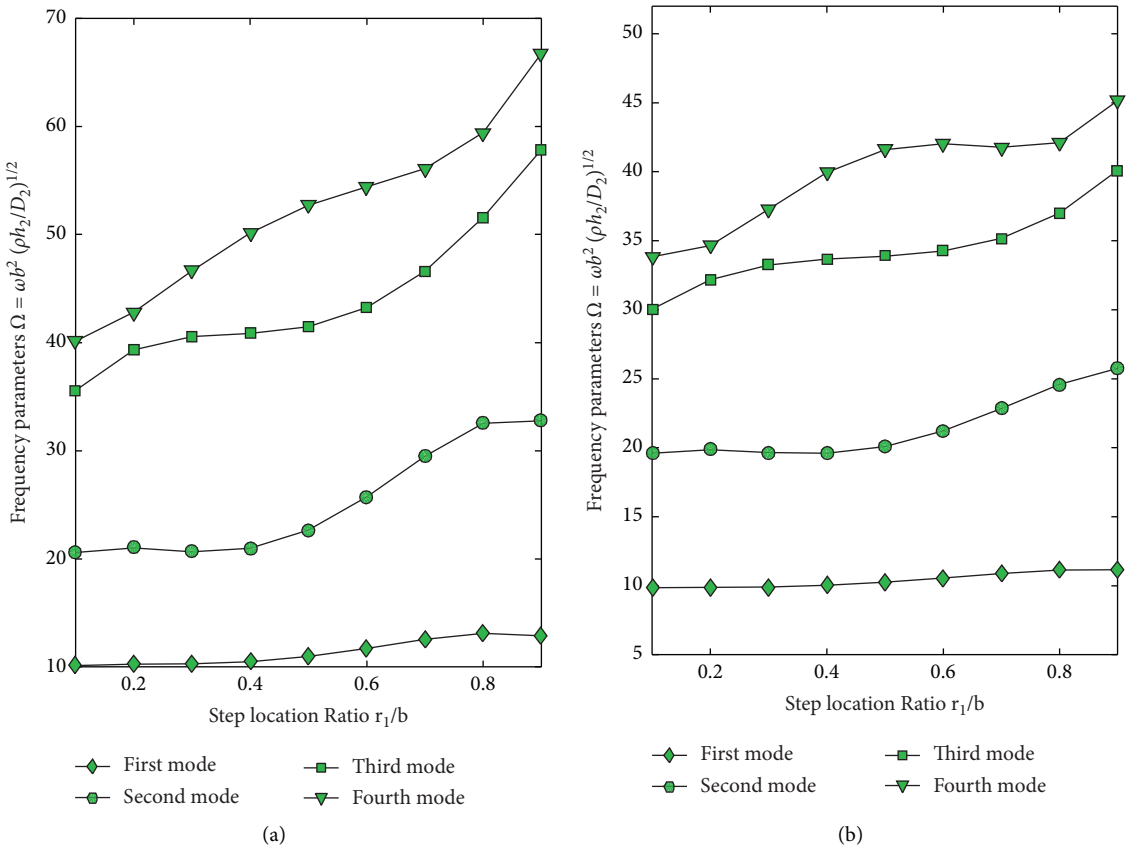

FIGURE 5: Frequency parameters $\Omega = \omega b^2 \sqrt{\rho h_2/D_2}$ versus step location ratio r_1/b for clamped stepped circular Mindlin plates, step thickness ratio $h_1/h_2 = 2$, and plate thickness ratios h_1/b = (a) 0.006 and (b) 0.15.

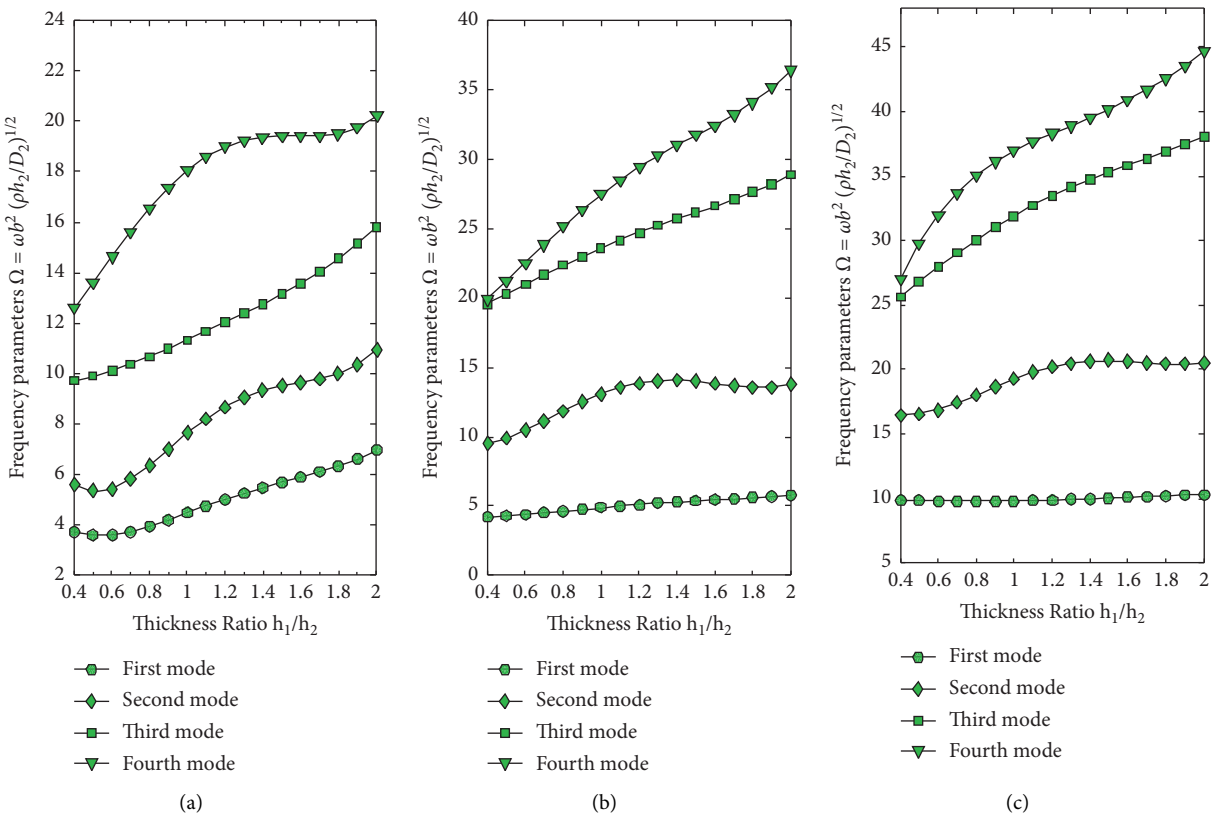

FIGURE 6: Frequency parameters $\Omega = \omega b^2 \sqrt{\rho h_2/D_2}$ versus step thickness ratio h_1/h_2 for stepped circular Mindlin plates (a) free, (b) simply supported, (c) clamped, step location ratio $r_1/b = 0.4$, and plate thickness ratio $h_1/b = 0.1$.

clamped and simply supported stepped circular plate firstly increase and then decrease with the variation of the step thickness ratio. Especially, the first frequency parameters for the first mode of the research model with simply supported and clamped boundary conditions present slight changes as the step ratio increases.

4. Conclusion

In this paper, a unified solution of the improved Fourier–Ritz method has been presented to solve the free vibration of stepped circular Mindlin plate with various kinds of boundary conditions. Under the current solution framework, the displacements of stepped circular Mindlin plate, regardless of the shapes and boundary conditions of the model, can be expressed as a special form of trigonometric series expansion with accelerated convergence. By comparing the results of the traditional calculation method by numerous numerical examples, the high accuracy and convergence of the current solution are validated. The influence of the step thickness ratios and the locations of the step variations of the current model on the frequency parameters are studied. This solution method can be extended to the static and dynamic problems of stepped circular plates and others. These parametric studies of stepped circular Mindlin plates should be very helpful for engineers in the mechanical engineering field.

Data Availability

This paper is a theoretical analysis of stepped circular plates, and the required data have been given in the paper.

Conflicts of Interest

The authors declare that they have no conflicts of interest.

Acknowledgments

The authors would like to thank the anonymous reviewers for their very valuable comments.

References

[1] A. S. Sayyad and Y. M. Ghugal, "On the free vibration analysis of laminated composite and sandwich plates: a review of recent literature with some numerical results," *Composite Structures*, vol. 129, pp. 177–201, 2015.

[2] K. A. Alhazza and A. A. Alhazza, "A review of the vibrations of plates and shells," *The Shock and Vibration Digest*, vol. 36, no. 5, pp. 377–395, 2004.

[3] A. K. Sharma and N. D. Mittal, "Review on stress and vibration analysis of composite plates," *Journal of Applied Sciences*, vol. 10, no. 23, pp. 3156–3166, 2010.

[4] J. Lee and L. A. Bergman, "The vibration of stepped beams and rectangular plates by an elemental dynamic flexibility method," *Journal of Sound and Vibration*, vol. 171, no. 5, pp. 617–640, 1994.

[5] J. A. Gallego Juárez, "Axisymmetric vibrations of circular plates with stepped thickness," *Journal of Sound and Vibration*, vol. 26, no. 3, pp. 411–IN2, 1973.
[6] Y. K. Cheung, *Finite Strip Method in Structural Analysis*, Elsevier, Amsterdam, Netherlands, 2013.
[7] S. J. Guo, A. J. Keane, and M. Moshrefi-Torbati, "Vibration analysis of stepped thickness plates," *Journal of Sound and Vibration*, vol. 204, no. 4, pp. 645–657, 1997.
[8] I. Chopra, "Vibration of stepped thickness plates," *International Journal of Mechanical Sciences*, vol. 16, no. 6, pp. 337–344, 1974.
[9] Y. Xiang and C. M. Wang, "Exact buckling and vibration solutions for stepped rectangular plates," *Journal of Sound and Vibration*, vol. 250, no. 3, pp. 503–517, 2002.
[10] Y. Xiang and L. Zhang, "Free vibration analysis of stepped circular Mindlin plates," *Journal of Sound and Vibration*, vol. 280, no. 3-5, pp. 633–655, 2005.
[11] G. Duan, X. Wang, and C. Jin, "Free vibration analysis of circular thin plates with stepped thickness by the DSC element method," *Thin-Walled Structures*, vol. 85, pp. 25–33, 2014.
[12] A. Ghannadiasl and M. Mofid, "Free vibration analysis of general stepped circular plates with internal elastic ring support resting on Winkler foundation by green function method," *Mechanics Based Design of Structures and Machines*, vol. 44, no. 3, pp. 212–230, 2016.
[13] D. R. Avalos, H. A. Larrondo, V. Sonzogni, and P. A. A. Laura, "A general approximate solution of the problem of free vibrations of annular plates of stepped thickness," *Journal of Sound and Vibration*, vol. 196, no. 3, pp. 275–283, 1996.
[14] N. Bhardwaj, A. P. Gupta, K. K. Choong, C. M. Wang, and H. Ohmori, "Transverse vibrations of clamped and simply-supported circular plates with two dimensional thickness variation," *Shock and Vibration*, vol. 19, no. 3, pp. 273–285, 2012.
[15] A. P. Gupta and N. Bhardwaj, "Free vibration of polar orthotropic circular plates of quadratically varying thickness resting on elastic foundation," *Applied Mathematical Modelling*, vol. 29, no. 2, pp. 137–157, 2005.
[16] I. Eshraghi, S. Dag, and N. Soltani, "Bending and free vibrations of functionally graded annular and circular microplates under thermal loading," *Composite Structures*, vol. 137, pp. 196–207, 2016.
[17] I. Eshraghi and S. Dag, "Forced vibrations of functionally graded annular and circular plates by domain-boundary element method," *ZAMM-Journal of Applied Mathematics and Mechanics/Zeitschrift für Angewandte Mathematik und Mechanik*, vol. 100, no. 8, Article ID e201900048, 2020.
[18] K. Y. Lam and G. Amrutharaj, "Natural frequencies of rectangular stepped plates using polynomial beam functions with subsectioning," *Applied Acoustics*, vol. 44, no. 4, pp. 325–340, 1995.
[19] S. M. Dickinson, "Comment on "natural frequencies of rectangular stepped plates using polynomial beam functions with subsectioning"," . *Applied Acoustics*, vol. 3, no. 47, pp. 275–277, 1996.
[20] S. Rajasekaran and A. J. Wilson, "Buckling and vibration of rectangular plates of variable thickness with different end conditions by finite difference technique," *Structural Engineering & Mechanics*, vol. 46, no. 2, pp. 269–294, 2013.
[21] D.-S. Cho, B. H. Kim, J.-H. Kim, N. Vladimir, and T.-M. Choi, "Simplified dynamic analysis of stepped thickness rectangular plate structures by the assumed mode method," *Proceedings of the Institution of Mechanical Engineers - Part M: Journal of Engineering for the Maritime Environment*, vol. 231, no. 1, pp. 177–187, 2017.
[22] M. Derakhshani, S. Hosseini-Hashemi, and M. Fadaee, "An analytical closed-form solution for free vibration of stepped circular/annular Mindlin functionally graded plate," 2018, http://arXiv.org/abs/1804.10583.
[23] W. L. Li, "Free vibrations of beams with general boundary conditions," *Journal of Sound and Vibration*, vol. 237, no. 4, pp. 709–725, 2000.
[24] D. Shi, Q. Wang, X. Shi, and F. Pang, "An accurate solution method for the vibration analysis of Timoshenko beams with general elastic supports," *Proceedings of the Institution of Mechanical Engineers - Part C: Journal of Mechanical Engineering Science*, vol. 229, no. 13, pp. 2327–2340, 2015.
[25] X. Shi, D. Shi, W. L. Li, and Q. Wang, "A unified method for free vibration analysis of circular, annular and sector plates with arbitrary boundary conditions," *Journal of Vibration and Control*, vol. 22, no. 2, pp. 442–456, 2016.
[26] W. L. Li, X. Zhang, J. Du, and Z. Liu, "An exact series solution for the transverse vibration of rectangular plates with general elastic boundary supports," *Journal of Sound and Vibration*, vol. 321, no. 1-2, pp. 254–269, 2009.
[27] X. Shi, D. Shi, and Z. Qin, "In-plane vibration analysis of annular plates with arbitrary boundary conditions," *The Scientific World Journal*, vol. 2014, Article ID 653836, 2014.
[28] D. Shi, X. Shi, and W. L. Li, "Vibration analysis of annular sector plates under different boundary conditions," *Shock and Vibration*, vol. 2014, Article ID 517946, 11 pages, 2014.
[29] X. Shi, C. Li, F. Wang, and F. Wei, "A unified formulation for free transverse vibration analysis of orthotropic plates of revolution with general boundary conditions," *Mechanics of Advanced Materials and Structures*, vol. 25, no. 2, pp. 87–99, 2018.